HHS Public Access

Author manuscript

Proc IFAC World Congress. Author manuscript; available in PMC 2017 December 12.

Published in final edited form as:

Proc IFAC World Congress. 2017 July ; 50(1): 13532–13537. doi:10.1016/j.ifacol.2017.08.2347.

State Estimation Under Correlated Partial Measurement Losses: Implications for Weight Control Interventions

Penghong Guo[*], **Daniel E. Rivera**[*], **Jennifer S. Savage**[**], and **Danielle S. Downs**[***]

[*]School for Engineering of Matter, Transport, and Energy, Arizona State University, Tempe, AZ 85281 USA

[**]Center for Childhood Obesity Research and the Department of Nutritional Sciences, Penn State University, University Park, PA, USA

[***]Exercise Psychology Laboratory, Department of Kinesiology, Penn State University, University Park, PA, USA

Abstract

The growing prevalence of obesity and related health problems warrants immediate need for effective weight control interventions. Quantitative energy balance models serve as powerful tools to assist in these interventions, as a result of their ability to accurately predict individual weight change based on reliable measurements of energy intake and energy expenditure. However, the data collected in most existing weight interventions is self-monitored; these measurements often have significant noise or experience losses resulting from participant non-adherence, which in turn, limits accurate model estimation. To address this issue, we develop a Kalman filter-based estimation algorithm for a practical scenario where on-line state estimation for weight, or energy intake/expenditure is still possible despite correlated partial data losses. To account for non-linearities in the models, an algorithm based on extended Kalman filtering is also developed for sequential state estimation in the presence of missing data. Simulation studies are presented to illustrate the performance of the algorithms and the potential benefits of these techniques in real-life interventions.

Keywords

Estimation; Filtering; Kalman filter; Extended Kalman filter; Intermittent measurements; Multiple missing measurements; Obesity; Interventions

1. INTRODUCTION

Obesity has become a worldwide health concern due to its high prevalence and related adverse health consequences. According to the National Health and Nutrition Examination Survey (NHANES) conducted in 2011–2012, the prevalence of being overweight or obese (OW/OB; defined as a body mass index [BMI] ≥ 25 kg/m^2) is 68.5% among adults in the US, including 34.9% of adults being considered as obese (BMI ≥ 30 kg/m^2) [Ogden et al. (2014)]. High BMI is significantly associated with increased risks of cardiovascular diseases, diabetes, and other clinical comorbidities [Bastien et al. (2014)]. Parental obesity

may affect the offspring obesity through heredity [Wu and Suzuki (2006)]. Therefore, there exists a great need for effective weight control interventions to prevent and reduce obesity.

Body weight change results from an imbalance between energy intake and energy expenditure. Weight loss is achieved when total energy input is less than total energy output, and vice versa. Hence, in most of the existing weight intervention efforts [Steinberg et al. (2013); Vesco et al. (2016)], weight control is managed by monitoring participants' dietary intake and caloric expenditure in addition to their weight change. Based on these measures, physicians can examine if participants meet their caloric goals, so that further health counseling advice can be provided. To better understand how individuals maintain or lose weight, dynamic energy balance models that can accurately predict weight change have been well established [Thomas et al. (2009); Guo et al. (2016)], which if used as tools to assist interventions, will help physicians with better assessing the outcomes of weight regulation and foster patient adherence to diet or exercise plans.

Accurate model prediction requires reliable measurements of the key determinants of energy balance [Hall et al. (2012)]. In real-life weight interventions, however, the data is usually self-reported or self-monitored by free-living participants via electronic devices, which produces significant noise in the data collection, along with missing data due to forgetfulness or lack of participant adherence to interventions. If a measurement is considered as physiologically implausible due to significant error, it has to be discarded for assessment, resulting in more data missingness. These limitations in the measured data might create an issue if an energy balance model is used for sequential weight prediction or real-time calculation of caloric intake/expenditure during an intervention. Therefore, estimation algorithms that can address random loss of measurements for online state estimation of these components are necessary in order to enable an uninterruptedly informative health guidance to participants throughout an intervention.

Motivated from this standpoint, a recursive Kalman filter (KF) based algorithm for real-time state estimation from randomly intermittent measurements is developed in this paper to cope with inevitable data loss during weight change interventions. The problem of Kalman filtering with intermittent measurements has been examined in many recent papers. In the study by Sinopoli et al. (2004), the random arrival of measurements is modeled as a Bernoulli process characterized by a binary probability parameter λ taking values of 0 or 1. When it comes to a missing data point, the estimator treats it as receiving a measurement consisting of noise alone. The results in Sinopoli et al. (2004) are based on the assumption that each set of measurements at a sampling time is either obtained in full or lost completely. During interventions, however, a participant may forget to take measures of just one or two determinants occasionally. This is common with long-duration interventions, in which measurements can be lost in a random fashion. Hence, partial data loss needs to be considered and incorporated in the formulation of the algorithm. Also note that, if one determinant fails to be measured on a given day, the measurements of other determinants are likely to be missing for that same day also. Consequently, the probability of measurement loss for individual components may be correlated with each other.

Liu and Goldsmith (2004) generalize the analysis by allowing partial loss of observations, where the measurement loss of each output element needs to be considered and modeled separately. However, the derivation of the Kalman filter updates with partial measurement losses in Liu and Goldsmith (2004) is limited to a system with only two output elements. In weight interventions, there are usually three or more major energy balance components that can be measured separately, such as weight, energy intake and physical activity. Thus as an extension to the two element study in Liu and Goldsmith (2004), we derive a general formula of the recursive algorithm for partial measurement losses in this paper to accommodate an arbitrary system with multiple output elements. Additionally, the analysis in Liu and Goldsmith (2004) assumes the probability distributions of the measurement losses to be independent with each other, that is, the intermittent measurements are described with two *i.i.d.* Bernoulli variables. In this work, the observation losses among different components can be mutually correlated and the correlation is reflected in the problem formulation with joint probability density functions. Such settings have been established and studied by Deshmukh et al. (2014). Similar derivation and analysis recently have been extended to non-linear systems for which the extended Kalman filtering (EKF) with intermittent observations is investigated [Ahmad and Namerikawa (2013); Hu et al. (2012)]. Inspired by these papers, we develop an EKF-based algorithm with correlated measurement losses to enable a broader application.

This paper is organized as follows. Section 2 derives the formula for the two filtering-based algorithms for real-time state estimation with partial measurement losses. In Section 3, simulation studies based on hypothetical participants for weight interventions are presented to illustrate the performance of the estimation algorithms. Section 4 gives a summary of our conclusions.

2. ESTIMATION ALGORITHMS

In this section, both the KF and EKF-based estimation approaches with partial measurement losses are introduced.

2.1 Kalman Filtering With Partial Measurement Losses

Consider a multiple-input multiple-output (MIMO) discrete time linear system model with three output elements. The state and measurement equations of the system are defined as follows:

$$x_{k+1}=\mathrm{A}\ \ \mathrm{x}_k+\mathrm{B}\ \ \mathrm{u}_k+\omega_k \quad (1a)$$

$$\underbrace{\begin{bmatrix} y_{1,k} \\ y_{2,k} \\ y_{3,k} \end{bmatrix}}_{y_k} = \underbrace{\begin{bmatrix} C_1 \\ C_2 \\ C_3 \end{bmatrix}}_{C} x_k + \underbrace{\begin{bmatrix} \nu_{1,k} \\ \nu_{2,k} \\ \nu_{3,k} \end{bmatrix}}_{\nu_k} \quad (1b)$$

where k is the sampling time; x_k, $\omega_k \in \mathbb{R}^n$ are the state and noise of the system, respectively; $u_k \in \mathbb{R}^p$ is the system input; $y_k, \nu_k \in \mathbb{R}^{\sum_{i=1}^{3} m_i}$ are the measurement and measurement noise with elements $y_{i,k}$, $\nu_{i,k} \in \mathbb{R}^{m_i}$, respectively; A, B, and C are the system matrices with appropriate dimensions. We assume that ω_k and $\nu_{i,k}$ are uncorrelated zero-mean Gaussian white noise with covariances of $Q \geq 0$ and $R_{ii} > 0$, respectively, that is $\omega_k \sim \mathcal{N}(0, Q)$ and $\nu_{i,k} \sim \mathcal{N}(0, R_{ii})$; R is the block-diagonal covariance matrix for ν_k with the matrices R_{ii} on the diagonal, written as $R = diag\{R_{11}, R_{22}, R_{33}\}$. For the system described per (1), we also assume that (A, B) is completely stabilizable and (A, C) completely detectable so that the error covariance of Kalman filter converges to a unique value in case of no measurement loss.

To incorporate measurement loss in the algorithm, we use the Bernoulli variable $\gamma_{i,k}$ to model the random arrivals of the measurements: $\gamma_{i,k}$ taking the value of 1 indicates the measurement of the corresponding element, $y_{i,k}$, has been successfully received at time k, whereas its value of 0 indicates a measurement loss. $\gamma_{i,k}$ is assumed to have known probability distributions. Here, in order to simulate real-life intervention conditions, we assume correlation exists among $\gamma_{1,k}$, $\gamma_{2,k}$, and $\gamma_{3,k}$. Thus, the joint probability density function of $\Pr(\gamma_{1,k}, \gamma_{2,k}, \gamma_{3,k})$ is used. Note that $\gamma_{i,k}$ assumes to be independent of $\gamma_{j,l}$ if $k \neq l$.

The loss of a measurement can be treated equivalently as receiving a measurement with infinite noise variance. In the presence of measurement loss, the statistical characteristics of measurement noise will change accordingly and cannot be fully described with $\nu_{i,k}$ in (1b). Thus, a second measurement noise term $\nu'_{i,k}$ is introduced and defined with $\nu'_{i,k} \sim \mathcal{N}(0, R'_{\mathrm{ii}})$, with $R'_{\mathrm{ii}} \to \infty$. $\nu'_{i,k}$ has the same structure and dimensions as $\nu_{i,k}$. Similarly, we have $\nu'_k = [\nu'^{T}_{1,k}\ \nu'^{T}_{2,k}\ \nu'^{T}_{3,k}]^T \sim \mathcal{N}(0, R')$ with $R' = \mathrm{diag}\{R'_{11}, R'_{22}, R'_{33}\}$.

With the augmentation of the variables $\gamma_{i,k}$ and $\nu'_{i,k}$, the measurement equation per (1b) can be redefined for a general case with observation losses as

$$\begin{bmatrix} y_{1,k} \\ y_{2,k} \\ y_{3,k} \end{bmatrix} = \begin{bmatrix} \gamma_{1,k}(C_1 x_k + \nu_{1,k}) \\ \gamma_{2,k}(C_2 x_k + \nu_{2,k}) \\ \gamma_{3,k}(C_3 x_k + \nu_{3,k}) \end{bmatrix} + \begin{bmatrix} (1-\gamma_{1,k})\nu'_{1,k} \\ (1-\gamma_{2,k})\nu'_{2,k} \\ (1-\gamma_{3,k})\nu'_{3,k} \end{bmatrix} = \underbrace{\begin{bmatrix} \gamma_{1,k}C_1 \\ \gamma_{2,k}C_2 \\ \gamma_{3,k}C_3 \end{bmatrix}}_{\tilde{C}_k} x_k + \underbrace{\begin{bmatrix} \gamma_{1,k}\nu_{1,k} + (1-\gamma_{1,k})\nu'_{1,k} \\ \gamma_{2,k}\nu_{2,k} + (1-\gamma_{2,k})\nu'_{2,k} \\ \gamma_{3,k}\nu_{3,k} + (1-\gamma_{3,k})\nu'_{3,k} \end{bmatrix}}_{\tilde{\nu}_k} \tag{2}$$

Note that the measurement equation now becomes time-varying and stochastic in nature, due to the time-varying matrix $\tilde{C}_k$ being a function of the random variables $\gamma_{i,k}$. The elements of the new noise vector follow $\tilde{\nu}_{i,k} \sim \mathcal{N}(0, \tilde{R}_{ii})$ with $\tilde{R}_{\mathrm{ii}} = \gamma_{i,k} R_{\mathrm{ii}} + (1-\gamma_{i,k}) R'_{\mathrm{ii}}$, leading to $\tilde{\nu}_k \sim \mathcal{N}(0, \tilde{R})$ with $\tilde{R} = diag\{\tilde{R}_{11}, \tilde{R}_{22}, \tilde{R}_{33}\}$. From here, we re-derive the Kalman filter algorithm based on the time-varying system as described per (1a) and (2).

Following the Kalman filtering approach, we define,

$$\hat{x}_{k|k} \triangleq \mathbb{E}[x_k|y_0^k, u_0^k, \gamma_0^k]$$

$$P_{k|k} \triangleq \mathbb{E}[(x_k - \hat{x}_{k|k})(x_k - \hat{x}_{k|k})^T|y_0^k, u_0^k, \gamma_0^k] \quad (3)$$

$$\hat{x}_{k+1|k} \triangleq \mathbb{E}[x_{k+1}|y_0^k, u_0^k, \gamma_0^k]$$

$$P_{k+1|k} \triangleq \mathbb{E}[(x_{k+1} - \hat{x}_{k+1|k})(x_{k+1} - \hat{x}_{k+1|k})^T|y_0^k, u_0^k, \gamma_0^k]$$

where x_k, $\hat{x}_{k|k}$, and $\hat{x}_{k+1|k}$ represent the true state, the *a posteriori* and *a priori* state estimate; $\hat{P}_{k|k}$ and $\hat{P}_{k+1|k}$ denotes the *a posteriori* and *a priori* error covariance matrix; $\gamma_k = [\gamma_{1,k}\ \gamma_{2,k}\ \gamma_{3,k}]^T$, $\gamma_0^k = \{\gamma_0, \cdots, \gamma_k\}$, and $y_0^k = \{y_0, \cdots, y_k\}$.

The prediction step of this KF based algorithm to compute $\hat{x}_{k+1}$ and $P_{k+1|k}$ uses the information from the state equation only, so it remains deterministic as in the classical Kalman filter:

$$\hat{x}_{k+1|k} = A\,\hat{x}_{k|k} + \mathrm{B}\ \ u_k + \omega_k \quad (4)$$

$$P_{k+1|k} = A\hat{P}_{k|k}A^T + Q$$

However, the correction step becomes stochastic due to its dependence on the observation process:

$$\hat{x}_{k+1|k+1} = \hat{x}_{k+1|k} + K_{k+1}(y_{k+1} - \tilde{C}_{k+1}\hat{x}_{k+1|k}) \quad (5)$$

$$P_{k+1|k+1} = P_{k+1|k} - K_{k+1}\tilde{C}_{k+1}P_{k+1|k}$$

where $K_{k+1} = P_{k+1|k}\tilde{C}_{k+1}^T(\tilde{C}_{k+1}P_{k+1|k}\tilde{C}_{k+1}^T + \tilde{R})^{-1}$ is the optimal Kalman gain computed by minimizing $P_{k+1|k+1}$.

Given the random set of γ_k at each sampling time k, we can expect that there exists $2^3 = 8$ possible scenarios for measurement loss: Specifically, the number of missing elements can range from 0 to 3, with 0 as the measurement set being completely received and 3 indicating

completely lost. The probability of each combination can be calculated from the joint probability function Pr($\gamma_{1,k}$, $\gamma_{2,k}$, $\gamma_{3,k}$). In the following, the Kalman filter update equations based on four possible scenarios is discussed.

Scenario 1: No Observation Loss—This is the case where $\gamma_k = [1\ 1\ 1]^T$. The measurement equation per (2) becomes the same as (1b) with $\tilde{C}_k = C$ and $\tilde{\nu}_k = \nu_k$, so the system becomes completely observable with the measurement noise covariance of R. Hence, the corrector equations remain the same as in the standard Kalman filter formulation, expressed as:

$$\hat{x}_{k+1|k+1} = \hat{x}_{k+1|k} + P_{k+1|k}C^T(\mathrm{CP}_{k+1|k}C^T + R)^{-1} \times (y_{k+1} - C\hat{x}_{k+1|k}) \quad (6)$$

$$P_{k+1|k+1} = P_{k+1|k} - P_{k+1|k}C^T(\mathrm{CP}_{k+1|k}C^T + R)^{-1} \times \mathrm{CP}_{k+1|k}$$

Scenario 2: Complete Observation Loss—The complete observation loss is mathematically modeled by $\gamma_k = [0\ 0\ 0]^T$, leading to the description of the system per (2) simplified as $y_k = \nu_k'$. The corrector equations are equivalent to (6) by assigning $C = \mathbf{0}$ and replacing R with $R' \to \infty$, which gives

$$\hat{x}_{k+1|k+1} = \hat{x}_{k+1|k} \quad (7)$$

$$P_{k+1|k+1} = P_{k+1|k}$$

Equation (7) shows that the corrector updates the state estimate by directly propagating the *a priori* estimate when the system is completely unobservable.

Scenario 3: Single Observation Loss—There are three possible cases to be discussed when a single observation is lost. Because of space limitations, only the derivation for the case of $\gamma_{1,k} = 0$, $\gamma_{2,k} = \gamma_{3,k} = 1$ is described in detail here. Before using (5), note that the following holds:

$$
\begin{aligned}
&\tilde{C}_k^T(\tilde{C}_k P_{k+1|k}\tilde{C}_k^T+\tilde{R})^{-1}\tilde{C}_k \\
&=\tilde{C}_k^T(\tilde{C}_k P_{k+1|k}\tilde{C}_k^T+R+\mathrm{diag}\{(R'_{11}-R_{11}),0,0\})^{-1}\tilde{C}_k \\
&=\tilde{C}_k^T\begin{bmatrix} 0 & 0 & 0 \\ 0 & \mathscr{M}_{22}-\mathscr{M}_{21}\mathscr{M}_{11}^{-1}\mathscr{M}_{12} & \mathscr{M}_{23}-\mathscr{M}_{21}\mathscr{M}_{11}^{-1}\mathscr{M}_{13} \\ 0 & \mathscr{M}_{32}-\mathscr{M}_{31}\mathscr{M}_{11}^{-1}\mathscr{M}_{12} & \mathscr{M}_{33}-\mathscr{M}_{31}\mathscr{M}_{11}^{-1}\mathscr{M}_{13} \end{bmatrix}\tilde{C}_k \\
&=\tilde{C}_k^T\begin{bmatrix} 0 & 0 \\ 0 & \left(\begin{bmatrix} C_2 \\ C_3 \end{bmatrix} P_{k+1|k}\begin{bmatrix} C_2 \\ C_3 \end{bmatrix}^T+\begin{bmatrix} R_{22} & 0 \\ 0 & R_{33} \end{bmatrix}\right)^{-1} \end{bmatrix}\tilde{C}_k \\
&=\begin{bmatrix} C_2 \\ C_3 \end{bmatrix}^T\left(\begin{bmatrix} C_2 \\ C_3 \end{bmatrix} P_{k+1|k}\begin{bmatrix} C_2 \\ C_3 \end{bmatrix}^T+\begin{bmatrix} R_{22} & 0 \\ 0 & R_{33} \end{bmatrix}\right)^{-1}\begin{bmatrix} C_2 \\ C_3 \end{bmatrix}
\end{aligned}
\tag{8}
$$

where $(\tilde{C}_k P_{k+1|k}\tilde{C}_k^T+R)^{-1}=\begin{bmatrix} \mathscr{M}_{11} & \mathscr{M}_{12} & \mathscr{M}_{13} \\ \mathscr{M}_{21} & \mathscr{M}_{22} & \mathscr{M}_{23} \\ \mathscr{M}_{31} & \mathscr{M}_{32} & \mathscr{M}_{33} \end{bmatrix}$. By combining (8) with (5), the update step for this case becomes

$$
\hat{x}_{k+1|k+1}=\hat{x}_{k+1|k}+P_{k+1|k}\begin{bmatrix} c_2 \\ c_3 \end{bmatrix}^T\left(\begin{bmatrix} c_2 \\ c_3 \end{bmatrix} P_{k+1|k}\begin{bmatrix} c_2 \\ c_3 \end{bmatrix}^T+\begin{bmatrix} R_{22} & 0 \\ 0 & R_{33} \end{bmatrix}\right)^{-1}\left(\begin{bmatrix} y_{2,k} \\ y_{3,k} \end{bmatrix}+\begin{bmatrix} c_2 \\ c_3 \end{bmatrix}\hat{x}_{k+1|k}\right)
$$

(9)

$$
P_{k+1|k+1}=P_{k+1|k}-P_{k+1|k}\begin{bmatrix} C_2 \\ C_3 \end{bmatrix}^T\left(\begin{bmatrix} C_2 \\ C_3 \end{bmatrix} P_{k+1|k}\begin{bmatrix} C_2 \\ C_3 \end{bmatrix}^T+\begin{bmatrix} R_{22} & 0 \\ 0 & R_{33} \end{bmatrix}\right)^{-1}\begin{bmatrix} C_2 \\ C_3 \end{bmatrix} P_{k+1|k}
$$

The mathematical analysis for the other two cases is quite similar. For an arbitrary case of single observation loss, the update step can be generalized as:

$$
\hat{x}_{k+1|k+1}=\hat{x}_{k+1|k}+P_{k+1|k}\begin{bmatrix} C_j \\ C_l \end{bmatrix}^T\left(\begin{bmatrix} C_j \\ C_l \end{bmatrix} P_{k+1|k}\begin{bmatrix} C_j \\ C_l \end{bmatrix}^T+\begin{bmatrix} R_{\mathrm{jj}} & 0 \\ 0 & R_{\mathrm{ll}} \end{bmatrix}\right)^{-1}\left(\begin{bmatrix} y_{j,k} \\ y_{l,k} \end{bmatrix}+\begin{bmatrix} C_j \\ C_l \end{bmatrix}\hat{x}_{k+1|k}\right)
$$

$$
P_{k+1|k+1}=P_{k+1|k}-P_{k+1|k}\begin{bmatrix} C_j \\ C_l \end{bmatrix}^T\left(\begin{bmatrix} C_j \\ C_l \end{bmatrix} P_{k+1|k}\begin{bmatrix} C_j \\ C_l \end{bmatrix}^T+\begin{bmatrix} R_{\mathrm{jj}} & 0 \\ 0 & R_{\mathrm{ll}} \end{bmatrix}\right)^{-1}\begin{bmatrix} C_j \\ C_l \end{bmatrix} P_{k+1|k}
$$

(10)

Scenario 4: Two Observation Losses—Similar derivation of the correction step for this scenario can be listed as shown in (8), leading to the update equations below,

$$\hat{x}_{k+1|k+1}=\hat{x}_{k+1|k}+P_{k+1|k}C_i^T(C_iP_{k+1|k}C_i^T+R_{\mathrm{ii}})^{-1}\times(y_{i,k+1}-C_i\hat{x}_{k+1|k})$$

$$P_{k+1|k+1}=P_{k+1|k}-P_{k+1|k}C_i^T(C_iP_{k+1|k}C_i^T+R_{\mathrm{ii}})^{-1}\times C_iP_{k+1|k} \quad (11)$$

Generalized Formulation for an Arbitrary System: Based on the detailed derivations of this Kalman filter based algorithm for a three-sensor system, it is possible to extend it to an arbitrary MIMO system with q separate output sensors, as described below:

$$x_{k+1}=\mathrm{A}\ \mathrm{x}_k+\mathrm{B}\ \mathrm{u}_k+\omega_k \quad (12a)$$

$$\underbrace{\begin{bmatrix} y_{1,k} \\ y_{2,k} \\ \vdots \\ y_{q,k} \end{bmatrix}}_{y_k}=\underbrace{\begin{bmatrix} \gamma_{1,k}C_1 \\ \gamma_{2,k}C_2 \\ \vdots \\ \gamma_{q,k}C_q \end{bmatrix}}_{\tilde{C}_k}x_k+\underbrace{\begin{bmatrix} \gamma_{1,k}\nu_{1,k}+(1-\gamma_{1,k})\nu'_{1,k} \\ \gamma_{2,k}\nu_{2,k}+(1-\gamma_{2,k})\nu'_{2,k} \\ \vdots \\ \gamma_{q,k}\nu_{q,k}+(1-\gamma_{q,k})\nu'_{q,k} \end{bmatrix}}_{\tilde{\nu}_k} \quad (12b)$$

where $\tilde{\nu}_k \sim \mathcal{N}(0, \tilde{R})$ with $\tilde{R}=\mathrm{diag}\{\tilde{R}_{\mathrm{ii}}=\gamma_{i,k}R_{\mathrm{ii}}+(1-\gamma_{i,k})R'_{\mathrm{ii}}, i=1, 2, \cdots, q\}$. The hypothesis of ($A$, B) being completely stabilizable and (A, C) completely detectable still holds for this system. It can be expected that there are 2^q possible scenarios for observation loss. Here, we define a notation of $X^-_{\mathbb{Z}_1,\mathbb{Z}_2}$ as a sub-matrix of $X \in \mathbb{R}^{q_1\times q_2}$ by deleting the rows of X as indexed in $\mathbb{Z}_1$ and the columns indexed in $\mathbb{Z}_2$, respectively. For an arbitrary sequence of measurements defined by $\mathbb{Z} = \{n_1, n_2, \cdots\}$ *or* $\{\phi\}$, where $n_1, n_2, \cdots \in \{1, 2, \cdots, q\}$, the generalized formulation for the update equations is expressed as below,

$$\hat{x}_{k+1|k+1}=\hat{x}_{k+1|k}+P_{k+1|k}\{C^-_{\mathbb{Z},\phi}\}^T(\{C^-_{\mathbb{Z},\phi}\}P_{k+1|k}\{C^-_{\mathbb{Z},\phi}\}^T+R^-_{\mathbb{Z},\mathbb{Z}})^{-1}(\{y_{k+1}\}^-_{\mathbb{Z},\phi}-\{C^-_{\mathbb{Z},\phi}\}\hat{x}_{k+1|k})$$

$$P_{k+1|k+1}=P_{k+1|k}-P_{k+1|k}\{C^-_{\mathbb{Z},\phi}\}^T(\{C^-_{\mathbb{Z},\phi}\}P_{k+1|k}\{C^-_{\mathbb{Z},\phi}\}^T+R^-_{\mathbb{Z},\mathbb{Z}})^{-1}\{C^-_{\mathbb{Z},\phi}\}P_{k+1|k} \quad (13)$$

2.2 Extended Kalman Filtering With Partial Measurement Losses

In case of a non-linear system, the extended Kalman filter needs to be considered. Here, we define a MIMO non-linear discrete-time system with q output sensors as described with the following equations:

$$x_{k+1}=f(x_k,u_k)+\omega_k \quad (14a)$$

$$\underbrace{\begin{bmatrix} y_{1,k} \\ y_{2,k} \\ \vdots \\ y_{q,k} \end{bmatrix}}_{y_k} = \underbrace{\begin{bmatrix} g_1(x_k,u_k) \\ g_2(x_k,u_k) \\ \vdots \\ g_q(x_k,u_k) \end{bmatrix}}_{g(x_k,u_k)} + \underbrace{\begin{bmatrix} \nu_{1,k} \\ \nu_{2,k} \\ \vdots \\ \nu_{q,k} \end{bmatrix}}_{\nu_k} \quad (14b)$$

where the deterministic nonlinear functions $f(x_k, u_k) : \mathbb{R}^n, \mathbb{R}^p \rightarrow \mathbb{R}^n$, and $h(x_k, u_k) : \mathbb{R}^n, \mathbb{R}^p \rightarrow \mathbb{R}^q$ are continuously differentiable at every x_k and u_k. Linearizing the model in (14) gives $A_k=\left.\frac{\partial f(x_k,u_k)}{\partial x_k}\right|_{\hat{x}_{k-1|k-1},u_k}$, and $C_k=\left.\frac{\partial g(x_k,u_k)}{\partial x_k}\right|_{\hat{x}_{k|k-1},u_k}$. For this system, (A_k, Q) is completely stabilizable and (A_k, C_k) completely detectable. The prediction step is the same as in the classical EKF:

$$\hat{x}_{k+1|k}=f(\hat{x}_{k|k},u_k) \quad (15)$$

$$P_{k+1|k}=A_k\hat{P}_{k|k}A_k^T+Q$$

The equations for the update step can be derived and they are the same as (13) except for matrix C replaced with C_k. With this generalized formulation, state estimation based on an arbitrary non-linear system is enabled in the presence of intermittent measurements.

3. NUMERICAL EXAMPLES

In this section, two simulation studies based on two different energy balance models are presented to illustrate the algorithms explained in the previous section. The energy balance model used in Section 3.1 is designed to predict weight change for general populations, while the model used in Section 3.2 is only for pregnant women and has been applied in an on-going intervention study on gestational weight gain control for OW/OB women.

3.1 Linear System With Intermittent Measurements

The linear energy balance model used in this example is based on the work in Thomas et al. (2009).We reformulate the model into the form as following:

$$\Delta W_k=K_1\mathrm{EI}_k+K_2\mathrm{PA}_k+K_2\mathrm{RMR}_k \quad (16)$$

where ΔW is the body weight change; EI is the energy intake; PA is the physical activity; RMR is the resting metabolic rate; K_1 and K_2 are the system gain parameters, the values of which can vary by gender and other factors. Here, all hypothetical participants are assumed to be females, leading to $K_1 = 1.67 \times 10^{-4}$ and $K_2 = -1.8 \times 10^{-4}$. The derivation for the values of the two gain parameters is elaborated in the Appendix. With this model, a Kalman filtering problem with correlated partial measurement losses is formulated for an intervention designed for a general female population.

In this hypothetical intervention, all the measurements are assumed to be self-reported or self-monitored. For the measurement of ΔW, it is assumed that the participants weigh themselves daily using smart digital scales. The measurement of EI is obtained daily from self-reported questionnaires: Automated Self-Administered 24-Hour Dietary Recall (ASA-24). PA is measured daily with a wrist-worn accelerometer (*Jawbone*). Since RMR is relatively stable, it can be measured less frequently as a weekly variable with a portable sensing device (*Breezing*). Due to the dynamic characteristics of RMR and the relatively high accuracy of its measurement, we define RMR as a certain input with zero-order hold performed between weekly measures. EI and PA are defined as the states to be estimated. With this setting, the system configuration is as follows: $x = [EI\ PA]^T$; $y = [\Delta W\ EI\ PA]^T$; $u = [RMR]$;

$$A=\begin{bmatrix} 1 & 0 \\ 0 & 1 \end{bmatrix};B=[1];C=\begin{bmatrix} K_1 & K_2 \\ 1 & 0 \\ 0 & 1 \end{bmatrix};Q=\begin{bmatrix} 10000 & 0 \\ 0 & 10000 \end{bmatrix},R=\begin{bmatrix} 0.01 & 0 & 0 \\ 0 & 10000 & 0 \\ 0 & 0 & 10000 \end{bmatrix}$$

. (A, B) and (A, C) are checked to confirm stabilizability and detectability respectively in case of no observation losses.

To test the algorithm on a hypothetical participant with frequent measurement losses, it is assumed that the output measurements for this participant are missing for one third of the intervention (66% availability only); Correlation exists in the loss of data as shown by the pre-defined arrival rates of the three output measurements (Table 1). The steps for the KF-based algorithm are summarized as below:

1. Initialize: Set $\hat{x}(0|0) = [EI_0\ PA_0]^T$, $P(0|0) = I$. EI_0 and PA_0 are baseline measurements.
2. Predict: see (4).
3. Update: see (13).

The performance of the algorithm for this hypothetical participant is presented in Fig. 1. It can be seen that the estimates of EI and PA "adapt" from given initial values and keep tracking the true values closely despite the presence of noise and missing data with the developed KF-based algorithm. The algorithm produces good weight gain predictions compared with the noise corrupted measurements. Note that the high arrival rates are required for the estimation error to remain bounded, which is illustrated using the root mean square error (*RMSE*) for EI estimates as shown by the bottom plot in Fig. 1. With a low arrival rate, the boundedness of the error cannot be guaranteed (shown in Fig. 2).

3.2 Nonlinear System With Intermittent Measurements

In this example, we consider the gestational energy balance model in Guo et al. (2016) where the maternal weight gain ΔW during pregnancy can be linearly modeled as a function of *EI, PA* and *RMR*. The model is in a similar form as (16), where K_1 and K_2 are categorized by maternal BMI and weight. Here, we assume a participant with pre-pregnancy weight of 95 kg and BMI of 31 kg/m^2. For this participant, the gain parameters according to Table I in Guo et al. (2016) are $K_1 = 2.119 \times 10^{-4}$, $K_2 = -2.35 \times 10^{-4}$. This model is being used for an on-going behavioral intervention to manage weight gain during pregnancy. In this intervention, energy intake, physical activity, and maternal weight are self-reported or self-monitored. Considering the cost and participant burdens for measuring *RMR*, we use a quadratic regression formula (Guo et al. (2016)) to dynamically model *RMR* as a function of *W* throughout the intervention:

$$\mathrm{RMR}_k = \mathrm{aW}_k^2 + \mathrm{bW}_k + c \quad (17)$$

where $a = 0.1976$; $b = -13.424$; $c = 1457.6$. This quadratic function brings non-linearities into the energy balance model if combined with (17). Note that (17) uses total weight W_k instead of weight change ΔW_k. Defining $\Delta W_k = W_k - W_{k-1}$, the discrete nonlinear model by combining (16) and (17) is described as below,

$$x_{k+1} = \begin{bmatrix} x_{1,k+1} \\ x_{2,k+1} \end{bmatrix} = \begin{bmatrix} f_1(x_k, u_k) \\ f_2(x_k, u_k) \end{bmatrix} + \omega_k \quad (18a)$$

$$y_k = x_k + \nu_k \quad (18b)$$

where $x = y = [W\ EI]^T$; $u = [PA + c]$;

$$f_1(x_k, u_k) = K_2 \mathrm{ax}_{1,k}^2 + (K_2 b + 1) x_{1,k} + K_1 x_{2,k} + K_2 u$$

$$f_2(x_k, u_k) = x_{2,k} \quad (19)$$

After the linearization of the model, the algorithm specified in Section 2.2 can be applied. Baseline *W* and *EI* measurements are used for initialization. Simulation results are presented in Fig. 3 to test the performance of the algorithm, where $Q = \begin{bmatrix} 0.1 & 0 \\ 0 & 10000 \end{bmatrix}, R = \begin{bmatrix} 0.1 & 0 \\ 0 & 10000 \end{bmatrix}$. It can be seen that given the probability of *EI* data loss being 0.5, the state estimation of *EI* keeps tracking the true values closely despite the presence of noise and measurement loss with the EKF-based algorithm. Note that the estimation error remains bounded for the given arrival rate.

4. CONCLUSIONS

To address the issue of significant measurement loss and noise in the data collection during weight interventions, a Kalman filter based algorithm that can provide optimal estimates in the presence of measurement noise and possible losses is developed. The Extended Kalman filter-based algorithm is also provided and demonstrated to deal with non-linear energy balance models. The algorithm shows good performance in the simulation studies, and shows great potential for used in actual intervention therapies.

Acknowledgments

Support for this work has been provided by the National Heart, Lung, and Blood Institute (NHLBI) through grant R01 HL119245. The opinions expressed in this article are the authors' own and do not necessarily reflect the views of NHLBI.

References

Ahmad H, Namerikawa T. Extended Kalman filter-based mobile robot localization with intermittent measurements. Systems Science & Control Engineering: An Open Access Journal. 2013; 1(1):113–126.

Bastien M, et al. Overview of epidemiology and contribution of obesity to cardiovascular disease. Progress in Cardiovascular Diseases. 2014; 56(4):369–381. [PubMed: 24438728]

Deshmukh S, Natarajan B, Pahwa A. State estimation over a lossy network in spatially distributed cyber-physical systems. IEEE Transactions on Signal Processing. 2014; 62(15):3911–3923.

Guo, P., Rivera, DE., Downs, DS., Savage, JS. Semi-physical identification and state estimation of energy intake for interventions to manage gestational weight gain; Proc Am Contrl Conf; 2016. p. 1271-1276.

Hall KD, Heymsfield SB, et al. Energy balance and its components: implications for body weight regulation. Am J of Clin Nutr. 2012; 95(4):989–994. [PubMed: 22434603]

Hu J, Wang Z, et al. Extended kalman filtering with stochastic nonlinearities and multiple missing measurements. Automatica. 2012; 48(9):2007–2015.

Liu X, Goldsmith A. Kalman filtering with partial observation losses. 43rd IEEE Conference on Decision and Control (CDC). 2004; 4:4180–4186.

Ogden CL, Carroll MD, et al. Prevalence of childhood and adult obesity in the United States, 2011–2012. JAMA. 2014; 311(8):806–814. [PubMed: 24570244]

Sinopoli B, Schenato L, et al. Kalman filtering with intermittent observations. IEEE Transactions on Automatic Control. 2004; 49(9):1453–1464.

Steinberg DM, Tate DF, et al. The efficacy of a daily selfweighing weight loss intervention using smart scales and email. Obesity. 2013; 21(9):1789–1797. [PubMed: 23512320]

Thomas DM, Ciesla A, et al. A mathematical model of weight change with adaptation. Mathematical Biosciences and Engineering. 2009; 6(4):873. [PubMed: 19835433]

Vesco KK, et al. One-year postpartum outcomes following a weight management intervention in pregnant women with obesity. Obesity. 2016; 24(10):2042–2049. [PubMed: 27670399]

Wu Q, Suzuki M. Parental obesity and overweight affect the bodyfat accumulation in the offspring: the possible effect of a highfat diet through epigenetic inheritance. Obesity Reviews. 2006; 7(2):201–208. [PubMed: 16629875]

APPENDIX

Derivation of the two gain coefficients in (16) is described in this section. The two-compartment energy balance model developed in Thomas et al. (2009) is:

$$\lambda_{\mathrm{FFM}}\, p_{\mathrm{FFM}} \frac{\mathrm{dFFM}(t)}{\mathrm{dt}} + \lambda_{\mathrm{FM}} \frac{\mathrm{dFM}(t)}{\mathrm{dt}} = \mathrm{EI}(t) - \mathrm{EE}(t) \quad (20)$$

where *EE* is the energy expenditure; *FFM* and *FM* represent the fat free mass and fat mass, respectively; these two body mass compositions have their respective energy densities of λ_{FFM} = 955.384 kcals/kg and λ_{FM} = 7165 kcals/kg; p_{FFM} is the proportion of *FFM*(*t*) being muscle tissue available for energy reserve, ranging from 0.3 to 0.5. Here, we pick the value of p_{FFM} as 0.4. A linear approximation of the relationship between total body weight (*W*) and *FM* was given in Thomas et al. (2009), where $W = \alpha\, FM + \beta$ with α = 1.32 for female. Combining this relationship with $W = FFM + FM$ and substituting into (20) gives an expression of the model with respect to *W* alone, as shown below:

$$K \frac{\mathrm{dW}(t)}{\mathrm{dt}} = \mathrm{EI}(t) - \mathrm{EE}(t) \quad (21)$$

where $K = \frac{\lambda_{\mathrm{FM}} + \lambda_{\mathrm{FFM}}\, p_{\mathrm{FFM}} (\alpha - 1)}{\alpha}$. Representing *EE* as $EE = PA + RMR + \delta\, EI$, where the non-volitional physical activity is neglected and $\delta\, EI$ represents the thermic effect of food with δ = 0.07, leads to the reformulated energy balance model shown in the following equation:

$$\frac{\mathrm{dW}(t)}{\mathrm{dt}} = K_1 \mathrm{EI}(t) + K_2 \mathrm{PA}(t) + K_2 \mathrm{RMR}(t) \quad (22)$$

where $K_1 = 1.67 \times 10^{-4}$ and $K_2 = -1.8 \times 10^{-4}$.

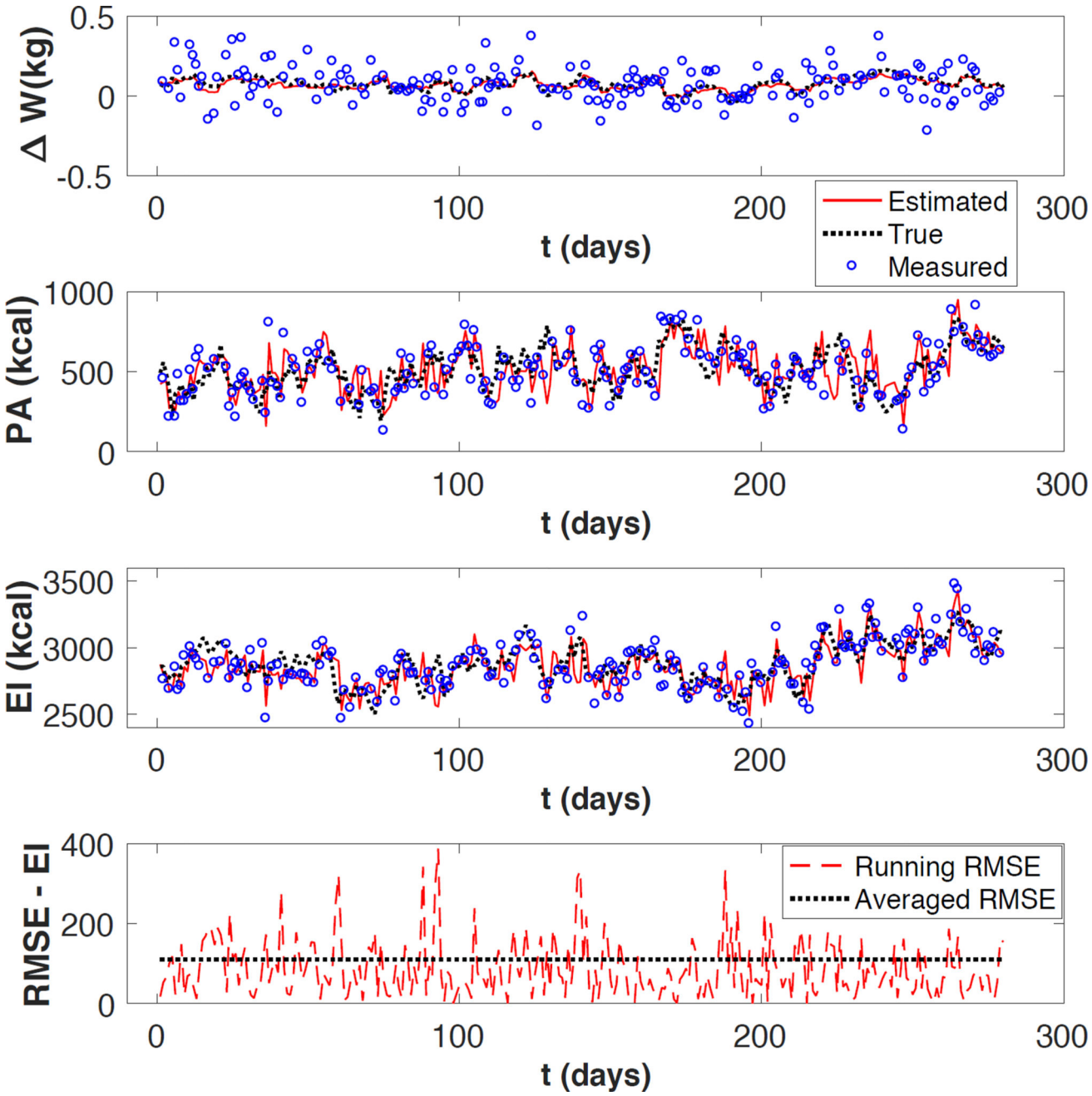

Fig. 1.

Performance of the KF algorithm illustrated using a hypothetical female participant with correlated partial measurement losses during an intervention.

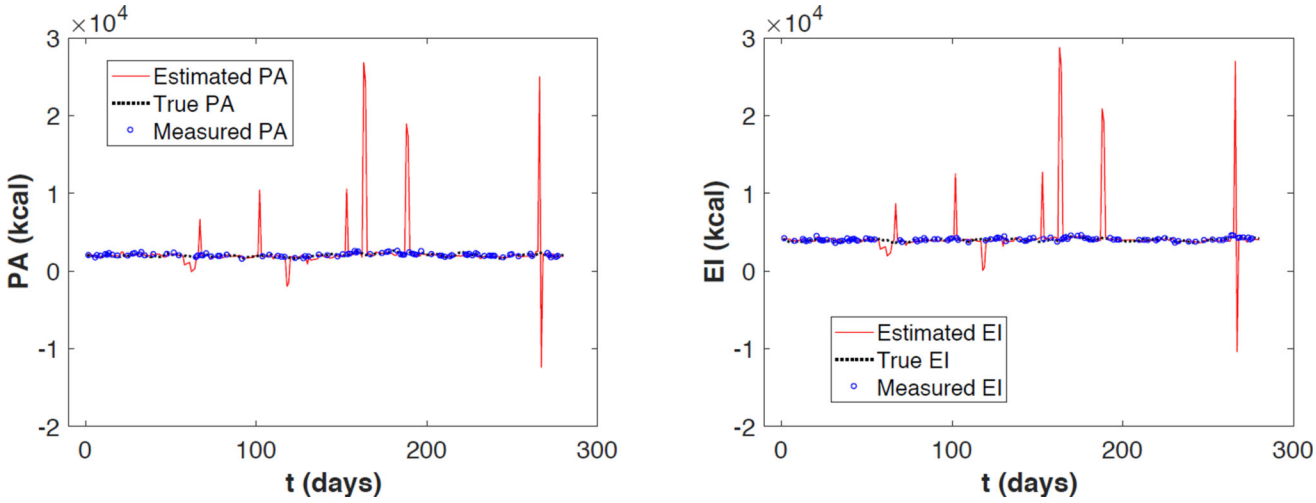

Fig. 2.
Simulation results with low arrival rates are shown to be divergent and unstable.

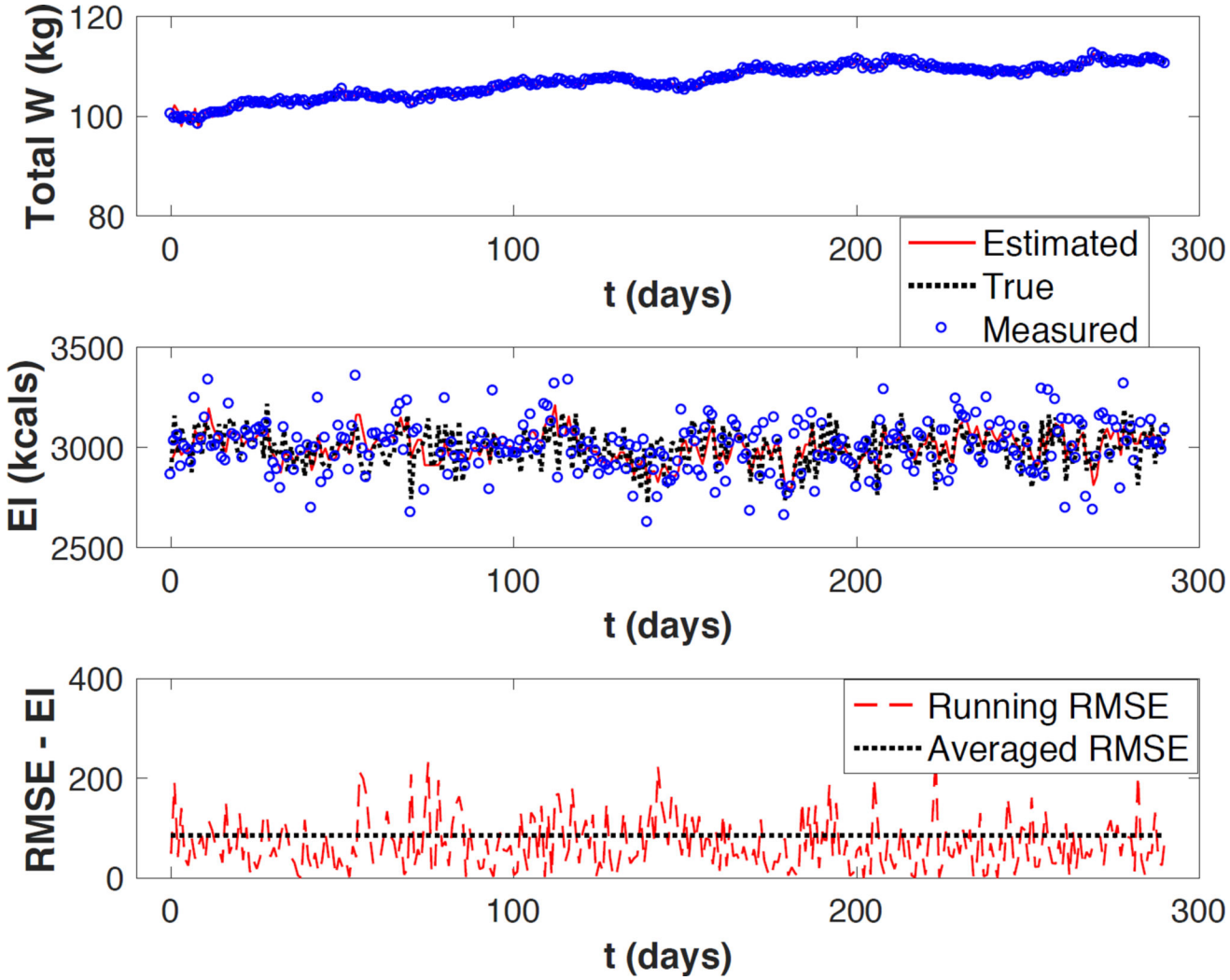

Fig. 3.

Performance of the EKF-based algorithm illustrated using a hypothetical participant in an intervention for gestational weight control.

Table 1

The joint probabilities of the measurement loss for a hypothetical participant. $\gamma_{1\sim3}$ indicate the arrival rates of the measurements for ΔW, *EI*, and *PA*, respectively.

Scenarios	$\gamma_3 = 0$		$\gamma_3 = 1$	
	$\gamma_2 = 0$	$\gamma_2 = 1$	$\gamma_2 = 0$	$\gamma_2 = 1$
$\gamma_1 = 0$	0.12	0.1	0.1	0.02
$\gamma_1 = 1$	0.1	0.02	0.02	0.52